


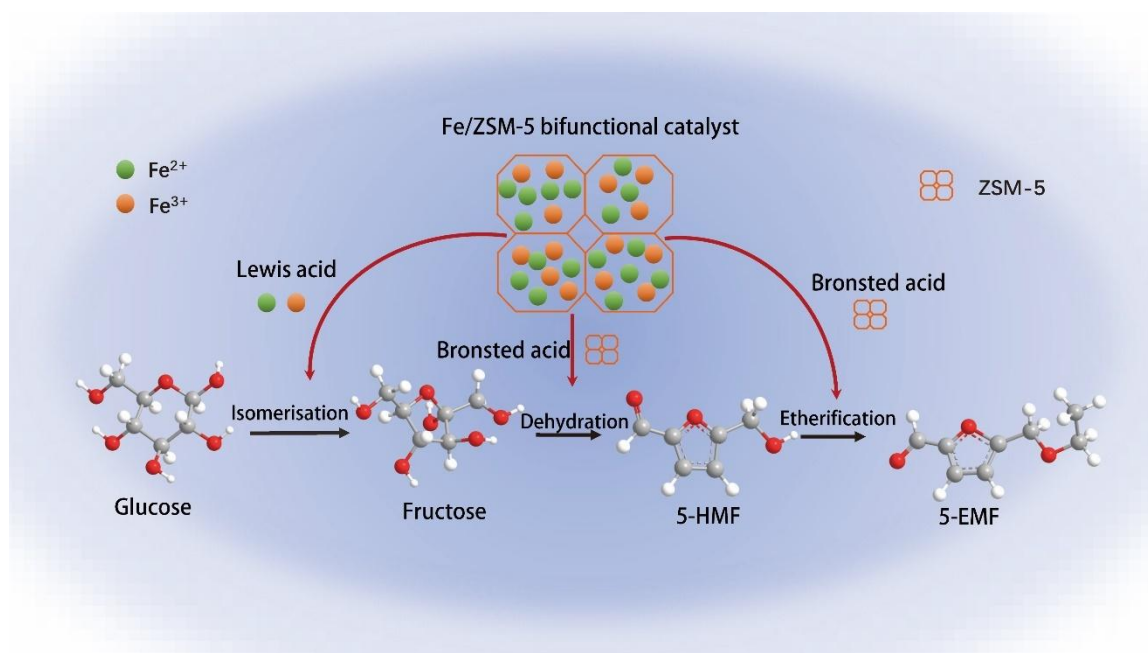
Production of 5-Ethoxymethylfurfural from Glucose Using Bifunctional Catalysts

Rui Zhang ^{a,*} Jiale Chen,^a Xishang Song,^a Jiantao Li,^a Jian Xiong,^b Zhihao Yu,^c and Xuebin Lu^b


* Corresponding author: rzhang@tcu.edu.cn

DOI: 10.15376/biores.20.2.2962-2978

GRAPHICAL ABSTRACT



Production of 5-Ethoxymethylfurfural from Glucose Using Bifunctional Catalysts

Rui Zhang ^{a,*} Jiale Chen,^a Xishang Song,^a Jiantao Li,^a Jian Xiong,^b Zhihao Yu,^c and Xuebin Lu^b

5-Ethoxymethylfurfural (5-EMF) is a promising liquid fuel or fuel additive due to its high energy density and stability. The conversion of glucose to 5-EMF involves a three-step tandem reaction: isomerization, dehydration, and etherification. However, low catalytic efficiency in these steps has limited 5-EMF yields. To address this, a Fe/ZSM-5 bifunctional catalyst with both Brønsted and Lewis acid sites was developed and characterized using XRD, SEM, XPS, BET, Py-FTIR, and NH₃-TPD techniques. The catalyst's performance in glucose conversion was systematically evaluated. Optimal conditions—20 wt% Fe loading, 180 °C reaction temperature, 10 h reaction time, and a catalyst-to-glucose mass ratio of 1:1—resulted in 97.1% glucose conversion and a 38.4% 5-EMF yield. Reaction kinetics followed a first-order model with an activation energy of 32.6 kJ/mol. The catalyst maintained over 94% glucose conversion after five cycles, demonstrating its stability. These findings underscore the potential of the Fe/ZSM-5 bifunctional catalyst for efficient glucose valorization to 5-EMF and provide key insights for process optimization.

DOI: 10.15376/biores.20.2.2962-2978

Keywords: Fe/ZSM-5 bifunctional catalyst; Isomerisation; Dehydration; Etherification; Glucose; 5-Ethoxymethylfurfural

Contact information: a: School of Environmental and Municipal Engineering, Tianjin Chengjian University, Tianjin 300384, China; b: School of Ecology and Environment, Tibet University, Lhasa 850000, China; c: School of Environmental Science and Engineering, Tianjin University, Tianjin 300350, China; *Corresponding author: rzhang@tcu.edu.cn

INTRODUCTION

With the global depletion of fossil fuel reserves, the expansion of renewable energy sources has become an urgent priority. The efficient utilization of lignocellulosic biomass presents a promising alternative to fossil fuels. As a major agricultural nation, China generates substantial amounts of agricultural waste annually, which serves as a significant source of lignocellulosic biomass (Zhao *et al.* 2024). Harnessing this resource is vital for promoting the transition to a sustainable energy structure. Lignocellulosic biomass primarily consists of cellulose, hemicellulose, and lignin. Among these components, cellulose is a linear, high-molecular-weight polysaccharide composed of repeating (1-4)- β -linked D-glucose units connected via β -1,4-glycosidic bonds. Hydrolysis of cellulose specifically cleaves these β -1,4-glycosidic bonds, liberating individual D-glucose molecules. These glucose units can subsequently be converted into biomass-derived platform chemicals, including 5-hydroxymethylfurfural (5-HMF), levulinic acid (LA), and γ -valerolactone (GVL), through further catalytic transformations (Mo *et al.* 2024). Notably, 5-HMF can be etherified to produce 5-ethoxymethylfurfural (5-EMF), a biomass-

derived compound with an energy density of 8.7 kWh/L, which is comparable to that of conventional gasoline (8.8 kWh/L) (Gawade *et al.* 2018). This makes 5-EMF a promising candidate for the development of next-generation biofuels, contributing to the diversification and sustainability of energy sources.

The development of efficient catalysts for the conversion of 5-HMF to 5-EMF is a critical challenge in this process. Sulfuric acid can be used as a catalyst to achieve a 5-EMF yield of 79.8% after 18 h of reaction at 70 °C (Yang *et al.* 2019). Che *et al.* (2012) employed H₄SiW₁₂O₄₀/MCM-41-loaded nanosphere catalysts with ethanol as the solvent, obtaining a 5-EMF yield of 77.2% after 4 h of reaction at 90 °C. These high yields were attributed to the effective design of the catalysts, where active components, such as metal oxides, were loaded onto zeolite carriers to enhance the yield and selectivity of the target products. Compared with zeolite-based solid acid catalysts, novel solid acid catalysts derived from carbonized biomass through sulfonation exhibit advantages such as improved biocompatibility and lower production costs (Rong *et al.* 2014). For instance, Yao *et al.* (2016) developed a sulfonated carbon-based solid acid catalyst, PCM-SO₃H-1, which facilitated the synthesis of 5-EMF from 5-HMF in a biphasic ethanol-dimethylsulfoxide system. Under optimized conditions (100 °C, 8 h), a maximum 5-EMF yield of 85.6% was achieved. While the direct synthesis of 5-EMF from 5-HMF achieves higher yields, the high cost of 5-HMF remains a significant barrier to the sustainable and cost-effective industrial production of 5-EMF. Therefore, developing more economical and efficient catalytic processes for the conversion of biomass-derived feedstocks to 5-EMF remains an area of active research.

Table 1. The Preparation of 5-EMF Catalyzed by Solid Acid Catalysts

Serial number	Catalysts	Solvent system	Substrate	Temperature (°C)	Time (h)	Yield (%)	Ref.
1	Glu-Fe ₃ O ₄ -SO ₃ H	Ethanol	HMF	80	2	92	Thombal <i>et al.</i> (2016)
2	Glu-Fe ₃ O ₄ -SO ₃ H	Ethanol	Fructose	80	24	81	Thombal <i>et al.</i> (2016)
3	Glu-Fe ₃ O ₄ -SO ₃ H	Ethanol /DMSO	Glucose	140	48	27	Thombal <i>et al.</i> (2016)
4	Glu-Fe ₃ O ₄ -SO ₃ H	Ethanol /DMSO	Fructose	100	12	85	Thombal <i>et al.</i> (2016)
5	OMC-SO ₃ H	Ethanol	Fructose	140	24	55.7	Wang <i>et al.</i> (2017)
6	OMC-SO ₃ H	Ethanol	Fructose	130	8	63.2	Wang <i>et al.</i> (2017)

The one-step conversion of glucose obtained from the hydrolysis of cellulose to 5-ethoxymethylfurfural (5-EMF) has become an important research priority. As summarized in Table 1, high yields of 5-EMF can be achieved when fructose is used as the reaction substrate. For instance, using a self-developed Glu-Fe₃O₄-SO₃H catalyst, researchers achieved an 81% yield of 5-EMF through a 24-hour catalytic reaction at 80 °C (Thombal *et al.* 2016). Similarly, Teeling *et al.* (2005) synthesized 5-EMF from fructose in an anhydrous phase using AlCl₃ as the catalyst, achieving a yield of 71.2%. Acidic ion-

exchange resins, such as Amberlyst-15, are widely employed in esterification and etherification reactions due to the presence of functional groups such as sulfonic acid (-SO₃H) and carboxylic acid (-COOH). Zuo *et al.* (2018) reported the use of commercial Amberlyst-15 ion exchange resin as a catalyst for the alcoholysis of fructose and inulin, achieving 5-EMF yields of 77.3% and 65.2%, respectively. When Amberlyst-15 was modified with chromium (Cr), the yields of 5-EMF were determined to be 46.7% and 50.2% when catalyzing glucose and sucrose, respectively (Son *et al.* 2012; EI-Nassan 2021). Although the yield of 5-EMF from glucose was lower compared to fructose, the significantly lower cost of glucose makes it a more viable feedstock for large-scale industrial applications. Consequently, the synthesis of 5-EMF from glucose has become a major area of research interest. In the one-pot synthesis process, glucose is initially isomerized to fructose *via* Lewis acid catalysis. The fructose is subsequently dehydrated to produce 5-HMF, catalyzed by Brønsted acid, followed by the etherification of 5-HMF with ethanol to form 5-EMF, also catalyzed by Brønsted acid (Wang *et al.* 2021; Zhang *et al.* 2022). However, the catalytic activity of existing catalysts is often insufficient for each step of this multistep reaction. This limitation is primarily attributed to the inappropriate ratio of Brønsted acid and Lewis acid sites in the catalysts. Therefore, the development of bifunctional catalysts with an optimal balance of Brønsted and Lewis acid sites is essential to enhance the efficiency and selectivity of the one-pot synthesis of 5-EMF from glucose.

In this study, an Fe/ZSM-5 bifunctional catalyst was developed to facilitate glucose isomerization (catalyzed by Lewis acid), dehydration (catalyzed by Brønsted acid), and etherification (catalyzed by Brønsted acid). The catalyst was designed to achieve efficient conversion of glucose to 5-EMF through the modulation of Brønsted and Lewis acid sites. The catalytic performance of the prepared Fe/ZSM-5 bifunctional catalysts was systematically evaluated, and their microphysical and chemical structures were thoroughly characterized. Furthermore, the reaction kinetics of glucose conversion to 5-EMF over the Fe/ZSM-5 bifunctional catalysts was investigated. This study will provide valuable insights into the catalytic behavior of bifunctional catalysts and offer a basis for optimizing multiphase catalytic systems for the conversion of glucose to 5-EMF.

EXPERIMENTAL

Materials

Concentrated sulphuric acid (analytically pure) was purchased from Tianjin Ruimingwei Chemical Co. Ltd, China. Analytically pure activated carbon, H-β zeolite, sodium hydroxide (NaOH), ferric chloride (FeCl₃), zirconium trichloride (ZrCl₃), copper chloride (CuCl₂), chromium trichloride (CrCl₃), ZSM-5 zeolite, guaranteed reagent of ethanol, dextrose, 5-EMF (99.9%), and phenolphthalein (99%) were purchased from Tianjin Biotest Technology Development Co. Ltd, China.

Catalyst Preparation

Four metal-loaded bifunctional catalysts (Zr, Cu, Fe, and Cr) supported on ZSM-5 molecular sieves were prepared separately using the wet impregnation method (Hoang *et al.* 2022). In this process, metal ions in an aqueous metal salt solution were mixed with a specific mass ratio of ZSM-5 zeolite. The mixture was then sonicated for 1 h and stirred at room temperature for 3 h. After impregnation, the mixture was dried at 105 °C for 12 h and ground into a fine powder. The resulting catalyst was then calcined in air at 550 °C for 6 h

with a linear temperature ramp of 2 °C/min. The final product was metal/ZSM-5 bifunctional catalyst containing both Brønsted and Lewis acid sites.

Characterisation of Catalysts

The crystalline phase of the samples was characterised by X-ray diffraction (XRD, Rigaku Smartlab 9KW, Japan) using a Rigaku Smartlab 9 KW, and analysed using MDI Jade 6.0.

Sample morphology was photographed using a high-resolution field emission scanning electron microscope (SEM, TESCAN MIRA LMS, Czech Republic) equipped with a Schottky field emission electron gun.

For quantitative and valence analysis of the elemental composition of the materials, X-ray photoelectron spectroscopy (XPS, Thermo Scientific K-Alpha, United States of America) was used to measure the inner electron binding energy of the atoms and their chemical shifts.

Fourier Transform Infrared Spectroscopy (FTIR, Nicolet is10, United States of America) test was used to characterize the molecular mechanism and chemical composition of materials. N₂ adsorption desorption experiments were performed on the catalysts using a TriStar II 30200 adsorption meter (BET, TriStar II 3020, United States of America).

The surface acid content of the catalysts were determined using a MicrotracBELCatII chemisorbentimeter (NH₃-TPD, Microtrac BELCat II, Japan).

Pyridine infrared spectroscopy (Bruker Tensor 27, German) was utilised to differentiate the acidity (Brønsted acid, Lewis acid) of the molecular sieve samples.

Catalytic Reaction

A reaction mixture consisting of 10 g/L glucose and a specific amount of catalyst was added to a 50 mL anhydrous ethanol solution in a flange mechanical stirring reactor. The procedure was to connect 99.99% N₂ in the inlet channel of the reactor, open the outlet channel of the reactor, pass high-purity nitrogen into the reactor uniformly, and maintain it for 15 min in order to exhaust the air in the reactor, and then close the outlet channel of the reactor until the pressure in the kettle reaches 0.1MPa to close the inlet channel of the reactor to begin the warming reaction. The catalytic conversion of glucose was then initiated at a reaction temperature of 140 °C and a reaction time of 5 min. Upon completion of the reaction, the reactor was immersed in cold water to cool. The products were filtered, diluted, and analyzed using high-performance liquid chromatography (HPLC, LC-20A, Japan) equipped with a refractive index detector. The analysis was performed using a BioRad Aminex HPX-87H column (300 × 7.8 mm) at 65 °C, with 5 mM H₂SO₄ as the mobile phase at a flow rate of 0.6 mL/min.

RESULTS AND DISCUSSION

Screening of Loaded Metal Catalysts

In the conversion of glucose to synthesize 5-EMF, glucose is first isomerized to fructose; this fructose is then dehydrated to produce 5-HMF, which is subsequently etherified to yield 5-EMF. The isomerization of glucose to fructose, however, is highly challenging under non-catalytic conditions (Dharmapriya and Huang 2024). Overcoming this critical step is essential to ensure efficient progression of the subsequent dehydration and etherification reactions. Without a catalyst, side reactions are more likely to dominate,

competing with the desired pathway and thereby reducing the yield of 5-EMF. Therefore, in the present study, metal-loaded bifunctional catalysts containing both Brønsted and Lewis acid sites were prepared by loading four metals (Zr, Cu, Fe, and Cr) onto ZSM-5 molecular sieves using the wet impregnation method. The catalytic performance of these catalysts was evaluated through the conversion of glucose too. As shown in Fig. 1, all four metal-loaded bifunctional catalysts successfully catalyzed the glucose conversion reaction, with glucose conversion yields exceeding 90%. Among them, the Fe/ZSM-5 bifunctional catalyst exhibited the best catalytic performance, with a 5-EMF yield of 30.8%. The Cu/ZSM-5, Zr/ZSM-5, and Cr/ZSM-5 bifunctional catalysts also promoted the synthesis of 5-EMF from glucose, but their catalytic activities were lower than that of Fe/ZSM-5 bifunctional catalyst. The lower activity of these three catalysts may be attributed to their inability to provide an adequate number of suitable Brønsted and Lewis acid sites, as well as an unfavorable distribution of these acid sites on the ZSM-5 molecular sieves. Based on these findings, the Fe/ZSM-5 bifunctional catalyst was selected for the catalytic conversion of glucose to 5-EMF in the subsequent study.

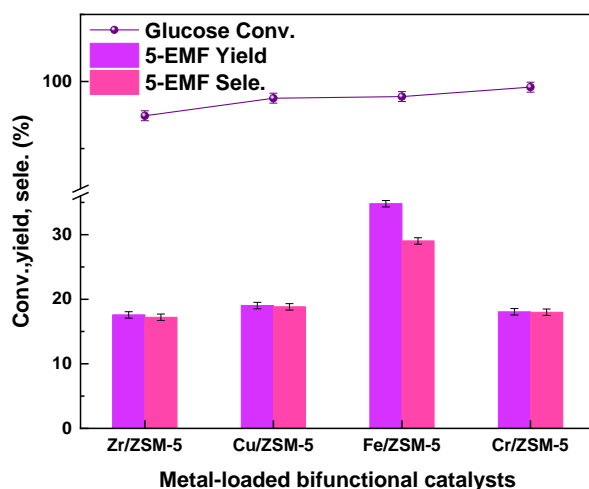


Fig. 1. Effect of different metal-loaded bifunctional catalysts on 5-EMF catalytic properties (glucose conversion, 5-EMF yield, 5-EMF selectivity) for glucose synthesis

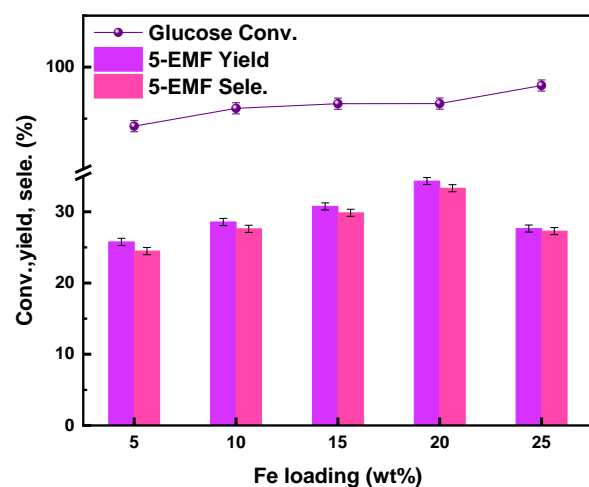


Fig. 2. Effect of Fe loading on the yield of 5-EMF (glucose 10 g/L, catalyst 10 g/L, reaction time 6 h, reaction temperature 180 °C)

Modulation of Catalytic Performance of Fe/ZSM-5 Bifunctional Catalysts

The ratio of Brønsted acid and Lewis acid sites on Fe/ZSM-5 bifunctional catalysts plays a crucial role in the isomerization of glucose to fructose, the dehydration of fructose to biomass-derived macromolecules, and the subsequent etherification reaction. This ratio can be effectively tuned by adjusting the metal loading on the ZSM-5 molecular sieves (Dutta *et al.* 2012). As shown in Fig. 2, the yield of 5-EMF initially increased and then decreased with increasing Fe loading, indicating that an optimal Fe loading is beneficial for glucose conversion. The best catalytic performance was observed when the Fe loading reached 20 wt.%, resulting in a 5-EMF yield of 34.4%. At this point, the ratio and number of Brønsted and Lewis acid sites on the Fe/ZSM-5 bifunctional catalyst were optimized (Liu *et al.* 2012; Jia *et al.* 2013).

The reaction temperature and reaction time are critical factors influencing the reaction rate and product distribution during glucose conversion. As shown in Fig. 3, within the temperature range of 140 to 220 °C, the glucose conversion rate steadily increased with temperature. When the temperature reached 180 °C, the yield of 5-EMF reached its maximum of 34.4%. However, although the glucose conversion rate continued to increase, the yield of 5-EMF began to decrease once the temperature exceeded 180 °C. This suggests that while moderate high temperatures promote glucose conversion to 5-EMF, excessively high temperatures lead to the formation of by-products that reduce the yield of 5-EMF. Therefore, 180 °C was selected as the optimal reaction temperature for further experiments.

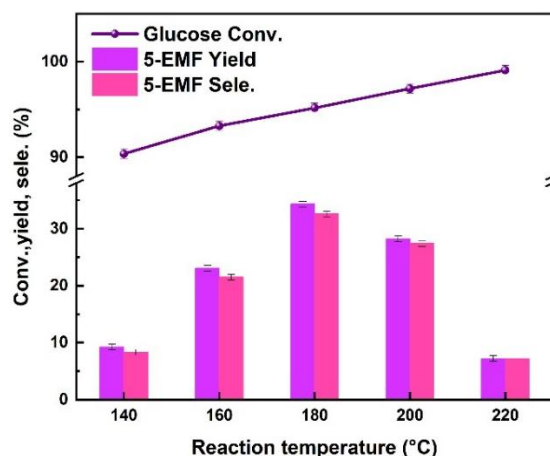


Fig. 3. Effect of reaction temperature on the yield of 5-EMF (glucose 10 g/L, catalyst 10 g/L, reaction time 6 h)

As shown in Fig. 4, the yield of 5-EMF exhibited an initial increase followed by a decrease within the reaction time range of 6 to 14 h. The yield of 5-EMF peaked at 38.2% when the reaction time reached 10 h. Beyond this point, the formation of by-products negatively impacted the yield of the target product, as reflected in the trend of 5-EMF selectivity. Based on these results, 10 h was determined to be the optimal reaction time.

The catalyst dosage is a crucial factor in evaluating the catalytic performance. As shown in Fig. 5, the glucose conversion steadily increased with the increase of Fe/ZSM-5 bifunctional catalyst dosage. However, the yield of 5-EMF peaked at a catalyst dosage of 0.5 g. Further increases in catalyst dosage resulted in a decrease in the 5-EMF yield, rather than an increase. This decrease may be due to the excess catalyst, which may have converted the 5-EMF into by-products, thus reducing the yield of the target product. Thus, 0.5 g of Fe/ZSM-5 bifunctional catalyst was selected as the optimal catalyst dosage.

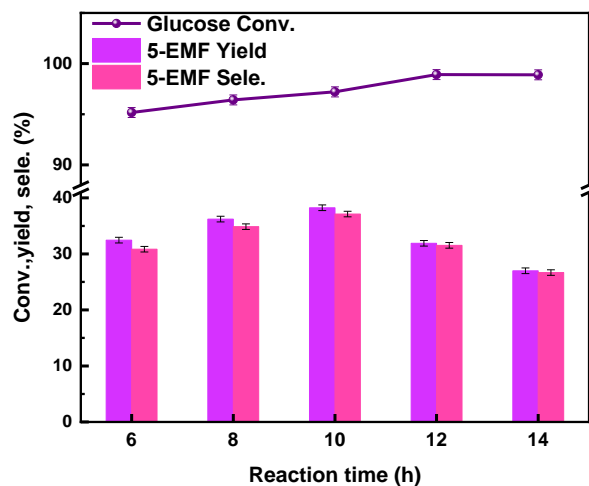


Fig. 4. Effect of reaction time on the yield of 5-EMF (glucose 10 g/L, catalyst 10 g/L, reaction temperature 180 °C)

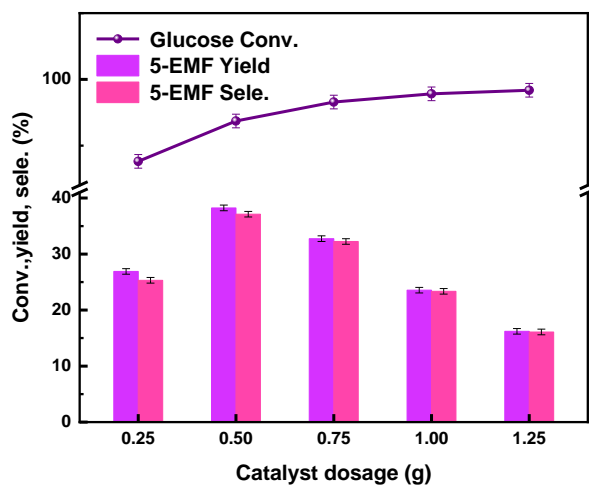


Fig. 5. Effect of catalyst dosage on the yield of 5-EMF (glucose 10 g/L, reaction temperature 180 °C, reaction time 10 h)

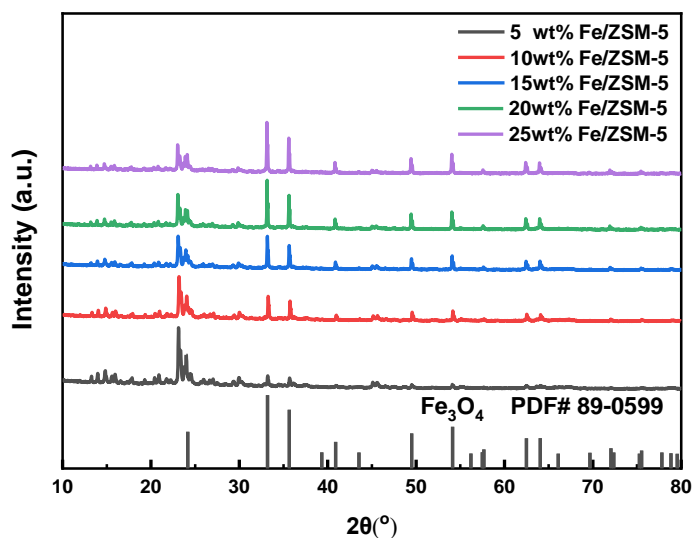


Fig. 6. X-ray diffraction (XRD) characterisation image of Fe/ZSM-5 bifunctional catalyst

Characterization of Fe/ZSM-5 Bifunctional Catalysts

The XRD characterization results (Fig. 6) indicate that the Fe/ZSM-5 bifunctional catalysts exhibited a series of peaks between 14° and 30° and around 45° , confirming that they retained the complete ZSM-5 (MFI) structure. Additionally, distinct peaks at approximately 24.2° , 33.2° , 35.7° , and 54.1° in the XRD pattern of the Fe/ZSM-5 bifunctional catalysts suggest that Fe_3O_4 was successfully loaded onto the ZSM-5 zeolite without disrupting its structure (Chen *et al.* 2020).

Further characterization of the Fe/ZSM-5 bifunctional catalysts was conducted using XPS to analyze elemental composition and chemical morphology. As shown in Fig. 7(a), the total energy spectrum displayed five characteristic peaks corresponding to Fe 2p, O 1s, C 1s, Si 2p, and Al 2p. The O 1s spectrum exhibited three sub-peaks between binding energies of 526.70 and 534.90 eV, corresponding to C-O bonds, C=O bonds, and a satellite peak, which is consistent with the fine mapping of the C1s spectrum. The fine mapping of Fe2p (1/2, 3/2) revealed two characteristic peaks near binding energies of 712 and 725.03 eV, indicating that the iron in the catalysts predominantly was present in the forms of Fe^{2+} and Fe^{3+} .

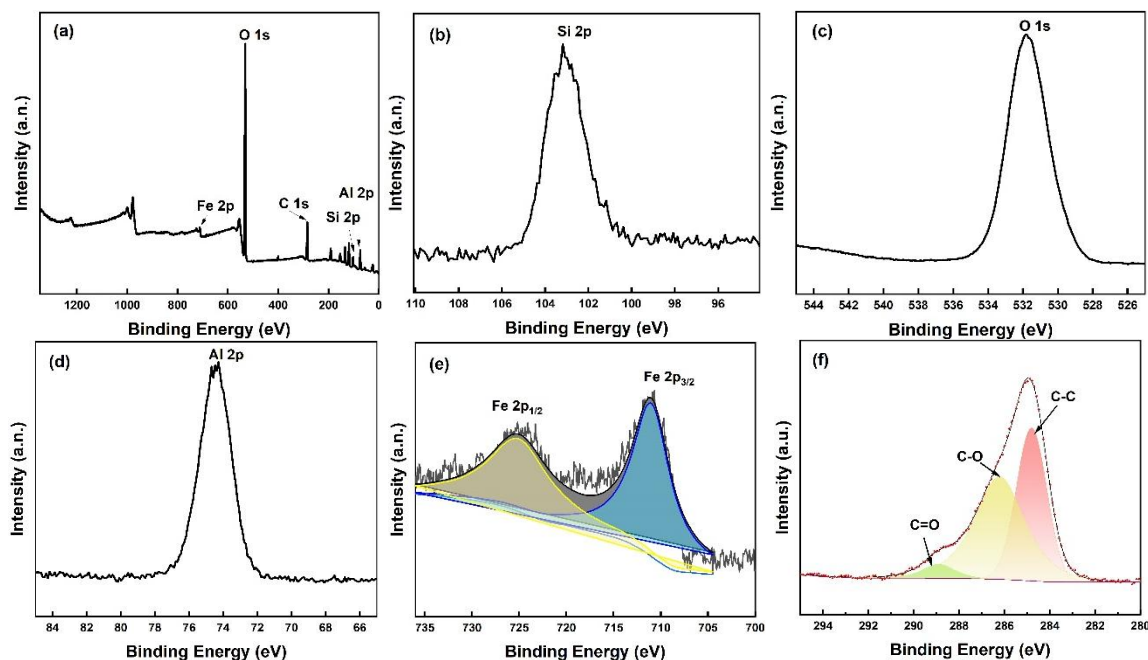


Fig. 7. X-ray photoelectron spectroscopy (XPS) characterisation image of Fe/ZSM-5 bifunctional catalyst

In this study, scanning electron microscopy (SEM) and energy dispersive spectroscopy (EDS) analyses were performed to examine the dispersion morphology and surface structure of the elements on the Fe/ZSM-5 bifunctional catalysts with varying metal loadings. As shown in Fig. 8, the loading of FeO did not significantly alter the surface properties of the carrier, and the crystal structure of ZSM-5 remained intact. However, agglomeration of metal ions was observed, which may lead to a decrease in surface area (Liu *et al.* 2018). The energy spectra (Fig. 8) revealed that the Fe elements were uniformly distributed on the catalyst surface. The best dispersion was observed at a 20 wt% Fe loading, which aligns with the experimental results. Fourier Transform Infrared Spectroscopy (FTIR) was employed to identify and analyze the chemical bonds and functional groups

present on the Fe/ZSM-5 bifunctional catalysts. The results (Fig. 9) showed vibrational peaks for surface hydroxyl groups and water molecules that were near 1630 cm^{-1} . Symmetric stretching absorption peaks for Al-O and Si-O chemical bonds appeared in the range of 450 to 800 cm^{-1} (Alam *et al.* 2018). A peak at 700 cm^{-1} was attributed to the Fe-O bond vibration (Wen *et al.* 2018; Kumar *et al.* 2019). Additionally, the peaks around 1100 cm^{-1} corresponded to the asymmetric stretching of Si-O-Al, Si-O-Si, and Al-O-Al bonds. A double-frequency peak at 1220 cm^{-1} was identified as the characteristic absorption of the five-membered ring of the ZSM-5 system (Yao *et al.* 2016). Overall, these findings further confirm that Fe was successfully loaded onto ZSM-5 without compromising its structural integrity.

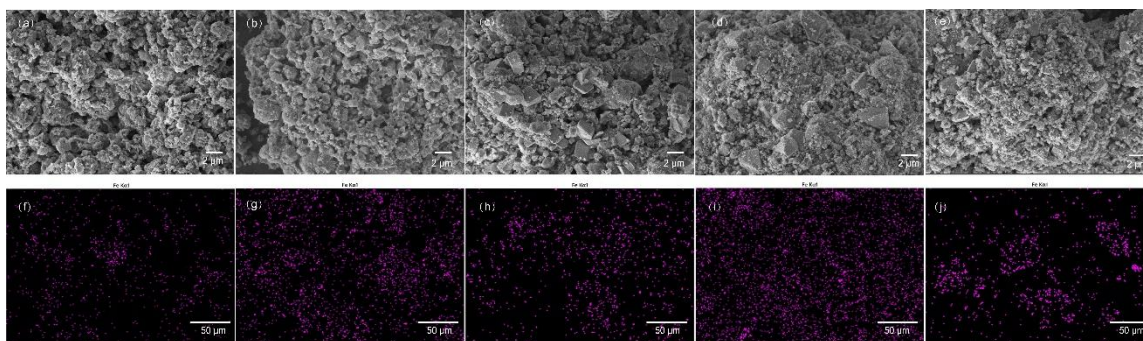


Fig. 8. Scanning electron microscopy and energy dispersive spectroscopy (SEM-EDS) characterisation images (a-e, SEM. f-j, EDS) of Fe/ZSM-5 bifunctional catalyst. (a) 5 wt%, (b) 10 wt%, (c) 15 wt%, (d) 20 wt%, (e) 25 wt%

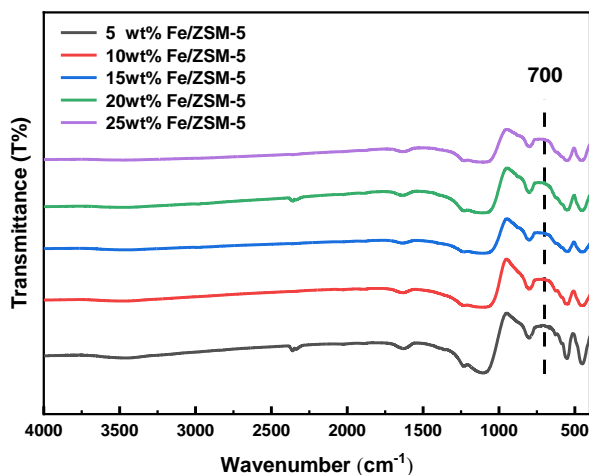


Fig. 9. FT-IR characterisation of Fe/ZSM-5 bifunctional catalyst

The N_2 adsorption-desorption isotherms are presented in Fig. 10. The results indicate that the isotherms of the Fe/ZSM-5 bifunctional catalysts with different Fe loadings all exhibited typical type IV adsorption curves. This behavior is indicative of nitrogen condensation during the medium pressure stage, which appeared as a H3-type hysteresis loop due to capillary condensation within the pores (Kumar *et al.* 2019). This suggests that all catalyst carriers possessed the characteristic structural features of slit-shaped mesoporous materials. The pore size distributions of the samples were obtained

through BJH analysis of the adsorption data (Fig. 10(b)). As shown in Table 2, an increase in Fe loading led to a decrease in both the specific surface area and pore size of the Fe/ZSM-5 bifunctional catalysts. In light of the catalytic performance data from the previous section, the optimal catalyst performance for 5-EMF yield was observed at a 20 wt.% Fe loading.

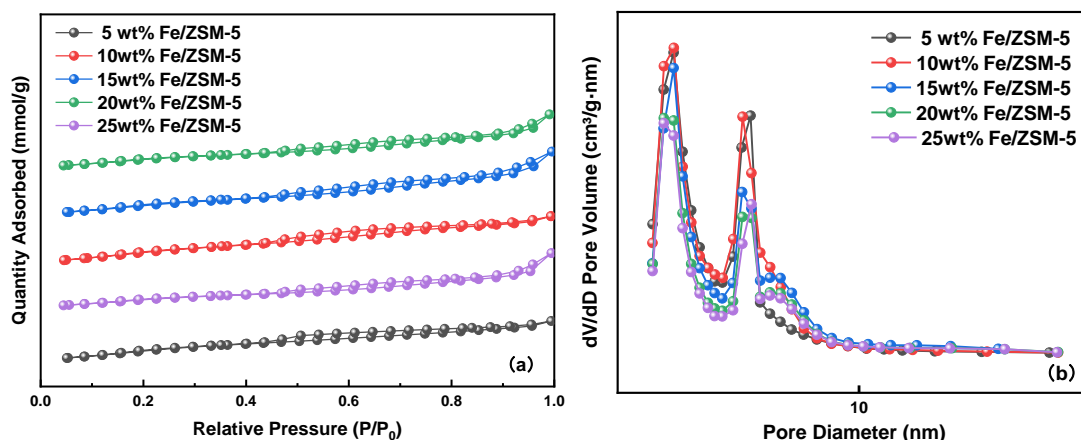


Fig. 10. Nitrogen adsorption-desorption characterization image of Fe/ZSM-5 bifunctional catalyst

Table 2. Specific Surface Area of Fe/ZSM-5 Bifunctional Catalysts with Different Loadings

Catalysts	Specific Surface Area (m ² /g)
5 wt% Fe/ZSM-5	254.16
10 wt% Fe/ZSM-5	249.53
15 wt% Fe/ZSM-5	232.36
20 wt% Fe/ZSM-5	206.97
25 wt% Fe/ZSM-5	194.43

The results from ammonia temperature-programmed desorption (NH₃-TPD) analysis (Fig. 11) show that the 20 wt% Fe/ZSM-5 bifunctional catalyst contained two types of acidic sites with varying acid strengths.

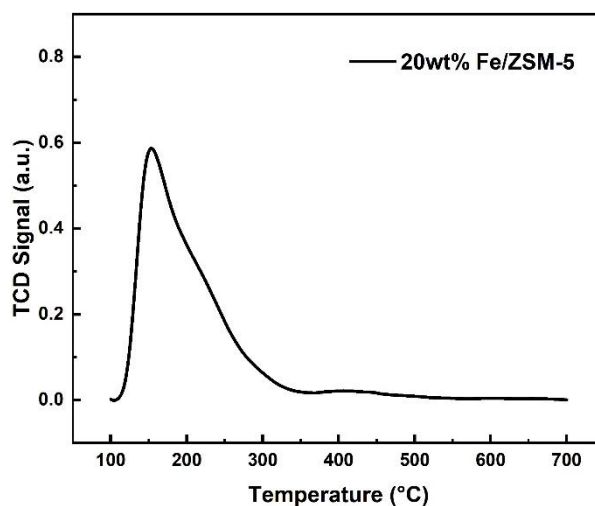


Fig. 11. Characterisation of ammonia programmed temperature rise desorption (NH₃-TPD)

The adsorption and desorption of NH_3 from the weakly acidic sites occurred within the temperature range of 110 to 250 °C, while the strongly acidic sites were observed in the range of 370 to 450 °C (Yu *et al.* 2024). Based on the ratio of the peak areas, the concentration ratio of weak to strong acidic sites on the Fe/ZSM-5 bifunctional catalyst surface was found to be 17:1. From the IR characterization, it can be inferred that the weak acidic sites on the catalyst surface are likely derived from -OH and -COOH groups on the catalyst support, while the strong acidic sites are attributed to the Lewis acid sites provided by the Fe species loaded onto the ZSM-5 zeolite. The total acidity of the Fe/ZSM-5 bifunctional catalysts was determined to be 0.87 mmol/g.

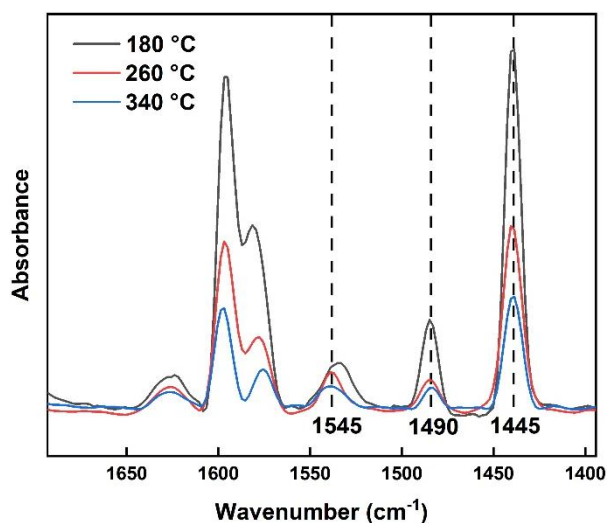


Fig. 12. Py-IR characterisation of Fe/ZSM-5 bifunctional catalyst

Figure 12 shows the Py-IR spectra of the Fe/ZSM-5 bifunctional catalysts at temperatures of 180, 260, and 340 °C. The pyridine adsorption peaks corresponding to the Lewis acid and Brønsted acid sites appeared around 1445 and 1545 cm^{-1} , respectively, while the peak near 1490 cm^{-1} resulted from the combination of both sites (Kumari *et al.* 2019). The acidic sites of the Fe/ZSM-5 bifunctional catalysts were primarily attributed to the Fe component within the framework, whereas Brønsted acidity was exclusively provided by the bridging hydroxyl group of Si-O-Fe (Trachta *et al.* 2022). The acid amount and distribution of the zeolite catalysts were calculated by combining the NH_3 -TPD and Py-IR characterization results (Table 3). The total acid amount of the Fe/ZSM-5 bifunctional catalyst decreased with increasing pyridine desorption temperature, indicating that the catalyst lost a portion of its acidic sites at higher temperatures.

Table 3. Acid Density of Fe/ZSM-5 Bifunctional Catalyst

Temperature (°C)	Brønsted acid area	Lewis acid area	Brønsted acid volume	Lewis acid volume	Total acid quantity	Brønsted acid / Lewis acid
180	0.45	2.07	18.506	63.861	82.367	0.290
260	0.33	1.28	13.347	39.584	52.932	0.337
340	0.17	0.672	6.755	20.782	27.537	0.325

Kinetic Analysis of Glucose Conversion to 5-EMF

Glucose dehydration reaction is a pseudo-first-order reaction, dependent on the concentrations of the reactants (Bounoukta *et al.* 2021). If the glucose dehydration reaction follows pseudo-first-order kinetics, a plot of $\ln(C_0/C)$ versus reaction time would be linear, with the slope equal to the negative value of the reaction rate constant (K) (Wang *et al.* 2015). To elucidate the reaction process, a simplified kinetic model for the macroscopic glucose alcoholysis reaction was proposed, as shown in Fig. 13.

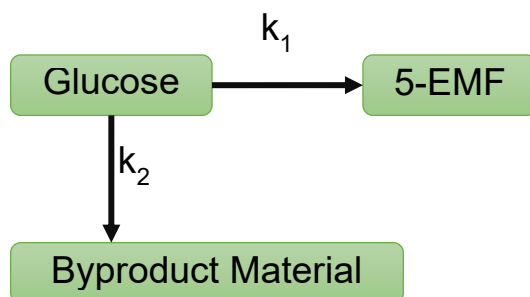


Fig. 13. Reaction kinetics model

The reaction process consisted of two main steps: (1) the conversion and synthesis of glucose to 5-EMF, and (2) the conversion of glucose into by-products. The glucose conversion and synthesis to 5-EMF was simplified into a single-stage reaction, and the corresponding differential equation was derived, as follows,

$$\frac{dC_G}{dt} = -(k_1 C_G + k_2 C_G) \quad (1)$$

$$C_G = C_{G0} e^{-kt} \quad (2)$$

$$\frac{dC_{5-EMF}}{dt} = k_2 C_G = k_2 (C_{G0} e^{-kt}) \quad (3)$$

$$k_1 + k_2 = k \quad (4)$$

$$Y_{5-EMF} = \frac{k_2}{k_1 + k_2} [1 - e^{-(k_1+k_2)t}] \quad (5)$$

where C_G is the concentration of glucose feedstock (g/L) and the initial concentration is denoted as C_{G0} ; C_{5-EMF} is the concentration of 5-EMF (g/L); Y_{5-EMF} is the yield of 5-EMF (mol%); k_1 and k_2 are the reaction rate constants for the formation of by-products and 5-EMF, respectively (h^{-1}); k is the rate constant for the degradation of glucose; and t is the reaction time.

Table 4. Reaction Rate Constants at Different Temperatures

Temperature ($^{\circ}\text{C}$)	k_1	k_2	K	R^2
160	0.0360	0.0370	0.0730	0.9726
180	0.0576	0.0610	0.1186	0.9855
200	0.0889	0.0712	0.1601	0.9730

The yield of 5-EMF (Y_{5-EMF}) obtained at different temperatures was substituted into Eq. 5, and the data were analyzed using MATLAB. The resulting kinetic parameters are

presented in Table 4. The value of the rate constant (k) increased with the rise of temperature, indicating that higher temperatures accelerated the formation of 5-EMF. This suggests that the reaction rate is enhanced at elevated temperatures, which is consistent with the results obtained from the temperature-dependent experiments. Additionally, the R^2 values of the fitted curves for the reaction kinetics at various temperatures, as shown in Fig. 14, further confirm that glucose dehydration follows first-order kinetics with a good fit.

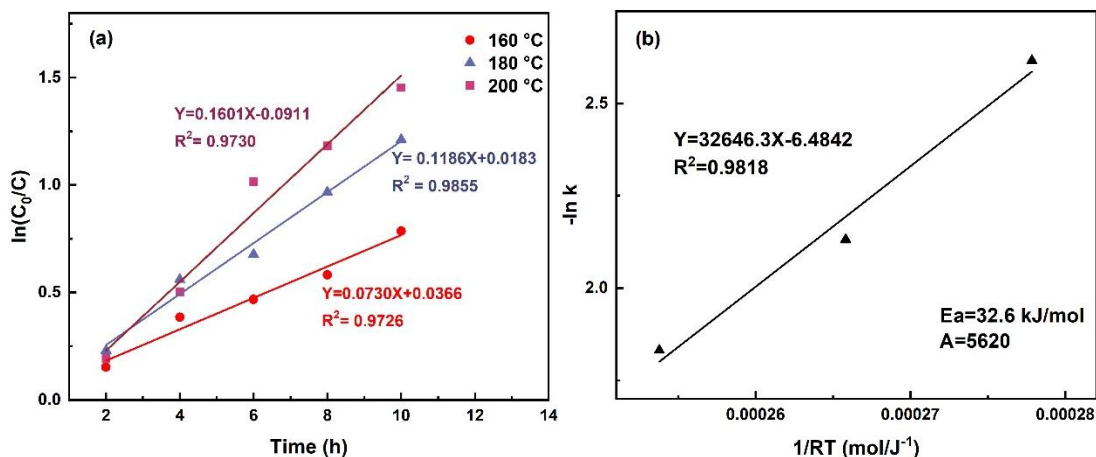


Fig. 14. Reaction kinetic curves and activation energy for glucose dehydration

The Arrhenius formula reveals the relationship between the rate of reaction and temperature in an exponential form (Eq. 6) and a logarithmic form (Eq. 7).

$$K_F = A_F e^{\left(-\frac{E_a}{RT}\right)} \quad (6)$$

$$\ln K_F = -\frac{E_a}{RT} + \ln A_F \quad (7)$$

Glucose dehydration is more consistent with a first-order kinetic reaction, and the activation energy curves were plotted and fitted with $1/RT$ as the horizontal coordinate and $-\ln k$ as the vertical coordinate. The activation energy E_a of the reaction with the participation of the Fe/ZSM-5 bifunctional catalyst was calculated to be 32.6 kJ/mol, with a pre-exponential factor $A = 5620 \text{ min}^{-1}$. The E_a values obtained in this study for the synthesis of 5-EMF from glucose catalyzed by the Fe/ZSM-5 bifunctional catalyst were lower than those values reported in the literature (64.2 to 73.2 kJ/mol) (Hsiao *et al.* 2021). This indicated that the Fe/ZSM-5 bifunctional catalyst is favorable for the conversion of glucose to 5-EMF.

Reusability of Fe/ZSM-5 Bifunctional Catalyst

To investigate the stability and reusability of Fe/ZSM-5 bifunctional catalysts, catalyst reuse experiments were conducted. In the ethanol reaction system, the catalytic glucose conversion reaction was carried out at 180 °C for 10 h. As shown in Fig. 15, after five cycles, the catalytic performance for glucose conversion remained stable, with conversion rates consistently above 94%. The yield of 5-EMF remained stable during the first four cycles, reaching 22.8% in the fifth cycle.

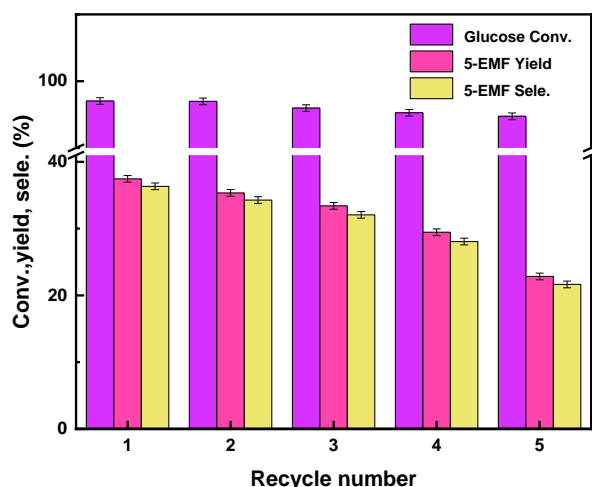


Fig. 15. Reusability of Fe/ZSM-5 bifunctional catalyst

Others

This study focused on the preparation of 5-EMF using pure glucose as the starting point for the reaction. Further challenges would need to be faced when cellulose is taken as the starting point, including a saccharification process to prepare crude glucose. The complexity of the substrate composition, the regulation of the reaction pathway, and other challenges should be considered when preparing 5-EMF from the glucose-rich crude fraction as the starting point. The glucose-rich crude fraction may contain lignin derivatives, organic acids, phenolic compounds, *etc.*, and the presence of these substances may affect the selectivity and yield of the reaction target. In addition, the presence of impurities is likely to cause side reactions, leading to a decrease in the yield of the target product. Future research, involving glucose-rich crude products, will be needed.

CONCLUSIONS

1. The optimum Fe/ZSM-5 bifunctional zeolite catalyst, with Fe loading 20 wt%, was determined through experimental optimization. Microstructural and chemical characterization revealed that the wet impregnation method did not alter the original structure of the ZSM-5 molecular sieves, and the Fe in the catalyst primarily was present in the forms of Fe^{2+} and Fe^{3+} . The yield of 5-EMF reached 38.2% with the optimal Fe/ZSM-5 bifunctional catalyst. The ratio of weak to strong acid sites on the catalyst surface was 17:1, indicating that the weak acid sites played a dominant role in the reaction.
2. The reaction kinetics of glucose dehydration followed a first-order kinetic model, and the addition of the catalyst significantly lowered the activation energy of the reaction. The activation energy for the Fe/ZSM-5 bifunctional catalyst in the reaction (32.6 kJ/mol) was lower than those values reported in the literature, indicating that the Fe/ZSM-5 bifunctional catalyst was favorable for catalyzing the conversion of glucose to 5-EMF.

3. The Fe/ZSM-5 bifunctional catalyst was easy to recycle and had catalytic activity with some effect. After five cycles, the conversion of glucose was always maintained above 94%, and the 5-EMF yield was maintained at 22.84%, which indicates the direction to optimize the Fe/ZSM-5 bifunctional catalyst in the future.

ACKNOWLEDGMENTS

This work was supported by the National Natural Science Foundation of China (Grant No. 51908400, 52066017, 51876180, 22308253), Tianjin Natural Science Foundation key project (23JCZDJC00430).

REFERENCES CITED

- Alam, Md. I., De, S., Khan, T. S., Haider, M. A., and Saha, B. (2018). "Acid functionalized ionic liquid catalyzed transformation of non-food biomass into platform chemical and fuel additive," *Ind. Crops Prod.* 123, 629-637. DOI: 10.1016/j.indcrop.2018.07.036
- Bounoukta, C. E., Megías-Sayago, C., Ammari, F., Ivanova, S., Monzon, A., Centeno, M. A., and Odriozola, J. A. (2021). "Dehydration of glucose to 5-hydroxymethylfurfural on bifunctional carbon catalysts," *Appl. Catal. B Environ.* 286, article ID 119938. DOI: 10.1016/j.apcatb.2021.119938
- Che, P., Lu, F., Zhang, J., Huang, Y., Nie, X., Gao, J., and Xu, J. (2012). "Catalytic selective etherification of hydroxyl groups in 5-hydroxymethylfurfural over H₄SiW₁₂O₄₀/MCM-41 nanospheres for liquid fuel production," *Bioresour. Technol.* 119, 433-436. DOI: 10.1016/j.biortech.2012.06.001
- Chen, B., Yan, G., Chen, G., Feng, Y., Zeng, X., Sun, Y., Tang, X., Lei, T., and Lin, L. (2020). "Recent progress in the development of advanced biofuel 5-ethoxymethylfurfural," *BMC Energy* 2(1), 2. DOI: 10.1186/s42500-020-00012-5
- Dharmapriya, T. N., and Huang, P.-J. (2024). "Exploring recent significant catalytic systems for the conversion of glucose into bio-based chemicals: A concise review," *Journal of the Taiwan Institute of Chemical Engineers* 162, article 105585. DOI: 10.1016/j.jtice.2024.105585
- Dutta, S., De, S., Alam, Md. I., Abu-Omar, M. M., and Saha, B. (2012). "Direct conversion of cellulose and lignocellulosic biomass into chemicals and biofuel with metal chloride catalysts," *J. Catal.* 288, 8-15. DOI: 10.1016/j.jcat.2011.12.017
- El-Nassan, H. B. (2021). "Amberlyst 15®: An efficient green catalyst for the synthesis of heterocyclic compounds," *Russ. J. Org. Chem.* 57(7), 1109-1134. DOI: 10.1134/S1070428021070125
- Gawade, A. B., and Yadav, G. D. (2018). "Microwave assisted synthesis of 5-ethoxymethylfurfural in one pot from d-fructose by using deep eutectic solvent as catalyst under mild condition," *Biomass Bioenergy* 117, 38-43. DOI: 10.1016/j.biombioe.2018.07.008
- Hoang, P. H., and Cuong, T. D. (2022). "Preparation of metal-loaded ZSM-5 zeolite catalyst and its catalytic effect on HMF production from biomass," *Appl. Biochem.*

- Biotechnol.* 194 (11), 4985-4998. DOI: 10.1007/s12010-022-03998-2
- Hsiao, C.-Y., Chiu, H.-Y., Lin, T.-Y., and Lin, K.-Y. A. (2021). "A comparative study on microwave-assisted catalytic transfer hydrogenation of levulinic acid to γ -valerolactone using Ru/C, Pt/C, and Pd/C," *Chem. Eng. Commun.* 208(11), 1511-1522. DOI: 10.1080/00986445.2020.1791833
- Huang, Y.-B., and Fu, Y. (2013). "Hydrolysis of cellulose to glucose by solid acid catalysts," *Green Chemistry*, 15(5), article 1095. DOI: 10.1039/c3gc40136g
- Jia, X., Ma, J., Che, P., Lu, F., Miao, H., Gao, J., and Xu, J. (2013). "Direct conversion of fructose-based carbohydrates to 5-ethoxymethylfurfural catalyzed by $\text{AlCl}_3 \cdot 6\text{H}_2\text{O} / \text{BF}_3 \cdot (\text{Et})_2\text{O}$ in ethanol," *J. Energy Chem.* 22 (1), 93-97. DOI: 10.1016/S2095-4956(13)60012-1
- Kumar, A., and Srivastava, R. (2019). "FeVO₄ decorated-SO₃H functionalized polyaniline for direct conversion of sucrose to 2,5-diformylfuran and 5-ethoxymethylfurfural and selective oxidation reaction," *Mol. Catal.* 465, 68-79. DOI: 10.1016/j.mcat.2018.12.017
- Kumari, P. K., Rao, B. S., Dhana Lakshmi, D., Sai Paramesh, N. R., Sumana, C., and Lingaiah, N. (2019). "Tungstophosphoric acid supported on mesoporous niobiumoxophosphate: An efficient solid acid catalyst for etherification of 5-hydroxymethylfurfural to 5-ethoxymethylfurfural," *Catal. Today.* 325, 53-60. DOI: 10.1016/j.cattod.2018.06.047
- Liu, J., Tang, Y., Wu, K., Bi, C., and Cui, Q. (2012). "Conversion of fructose into 5-hydroxymethylfurfural (HMF) and its derivatives promoted by inorganic salt in alcohol," *Carbohydr. Res.* 350, 20-24. DOI: 10.1016/j.carres.2011.12.006
- Liu, X., and Wang, R. (2018). "Upgrading of carbohydrates to the biofuel candidate 5-ethoxymethylfurfural (EMF)," *Int. J. Chem. Eng.* 2018, 1-10. DOI: 10.1155/2018/2316939
- Mo, S., Zheng, Y., Gong, J., and Lu, M. (2024). " γ -Valerolactone/CuCl₂ biphasic system for high total monosaccharides recovery from pretreatment and enzymatic hydrolysis processes of eucalyptus," *Front. Chem. Sci. Eng.* 18(11), article 139. DOI: 10.1007/s11705-024-2490-5
- Rong, Z., Sun, Z., Wang, L., Lv, J., Wang, Y., and Wang, Y. (2014). "Efficient conversion of levulinic acid into γ -valerolactone over Raney Ni catalyst prepared from melt-quenching alloy," *Catal. Lett.* 144(10), 1766-1771. DOI: 10.1007/s10562-014-1310-9
- Son, P. A., Nishimura, S., and Ebitani, K. (2012). "Synthesis of levulinic acid from fructose using Amberlyst-15 as a solid acid catalyst," *React. Kinet. Mech. Catal.* 106 (1), 185-192. DOI: 10.1007/s11144-012-0429-1
- Teeling, E. C., Springer, M. S., Madsen, O., Bates, P., O'Brien, S. J., and Murphy, W. J. (2005). "A molecular phylogeny for bats illuminates biogeography and the fossil record," *Science* 307(5709), 580-584. DOI: 10.1126/science.1105113
- Thombal, R. S., and Jadhav, V. H. (2016). "Application of glucose derived magnetic solid acid for etherification of 5-HMF to 5-EMF, dehydration of sorbitol to isosorbide, and esterification of fatty acids," *Tetrahedron Letters*, 57(39), 4398-4400. DOI: 10.1016/j.tetlet.2016.08.061
- Trachta, M., Bulánek, R., Bludský, O., and Rubeš, M. (2022). "Brønsted acidity in zeolites measured by deprotonation energy," *Sci. Rep.* 12(1), 7301. DOI: 10.1038/s41598-022-11354-x

- Wang, J., Zhang, Z., Jin, S., and Shen, X. (2017) "Efficient conversion of carbohydrates into 5-hydroxymethylfurfural and 5-ethoxymethylfurfural over sulfonic acid-functionalized mesoporous carbon catalyst," *Fuel*. 192, 102-107. DOI: 10.1016/j.fuel.2016.12.027
- Wang, J., Zhao, H., Zhu, B., Larter, S., Cao, S., Yu, J., Kibria, M. G., and Hu, J. (2021). "Solar-driven glucose isomerization into fructose via transient Lewis acid-base active sites," *ACS Catal.* 11(19), 12170-12178. DOI: 10.1021/acscatal.1c03252
- Wang, T., Glasper, J. A., and Shanks, B. H. (2015). "Kinetics of glucose dehydration catalyzed by homogeneous Lewis acidic metal salts in water," *Appl. Catal. Gen.* 498, 214-221. DOI: 10.1016/j.apcata.2015.03.037
- Wen, Y., Yu, Z., Li, K., Guo, H., Dai, Y., and Yan, L. (2018). "Fabrication of biobased heterogeneous solid Brønsted acid catalysts and their application on the synthesis of liquid biofuel 5-ethoxymethylfurfural from fructose," *Green Energy Environ* 3(4), 384-391. DOI: 10.1016/j.gee.2018.07.003
- Yang, F., Tang, J., Ou, R., Guo, Z., Gao, S., Wang, Y., Wang, X., Chen, L., and Yuan, A. (2019). "Fully catalytic upgrading synthesis of 5-ethoxymethylfurfural from biomass-derived 5-hydroxymethylfurfural over recyclable layered-niobium-molybdate solid acid," *Appl. Catal. B Environ.* 256, article ID 117786. DOI: 10.1016/j.apcatb.2019.117786
- Yao, Y., Gu, Z., Wang, Y., Wang, H.-J., and Li, W. (2016). "Magnetically-recoverable carbonaceous material: An efficient catalyst for the synthesis of 5-hydroxymethylfurfural and 5-ethoxymethylfurfural from carbohydrates," *Russ. J. Gen. Chem.* 86(7), 1698-1704. DOI: 10.1134/S1070363216070276
- Yu, N., Lu, H., Yang, W., Zheng, Y., Hu, Q., Liu, Y., Wu, K., and Liang, B. (2024). "Transfer hydrogenation of levulinic acid to γ -valerolactone over acid site-modified CuNi alloy," *Biomass Convers. Biorefinery* 14(7), 8271-8282. DOI: 10.1007/s13399-022-02887-2
- Zhang, H., Zhao, H., Zhai, S., Zhao, R., Wang, J., Cheng, X., Shiran, H. S., Larter, S., Kibria, M. G., and Hu, J. (2022). "Electron-enriched Lewis acid-base sites on red carbon nitride for simultaneous hydrogen production and glucose isomerization," *Appl. Catal. B Environ.* 316, article ID 121647. DOI: 10.1016/j.apcatb.2022.121647
- Zhao, X., Li, R.-C., Liu, W.-X., Liu, W.-S., Xue, Y.-H., Sun, R.-H., Wei, Y.-X., Chen, Z., Lal, R., Dang, Y. P., Xu, Z.-Y., and Zhang, H.-L. (2024). "Estimation of crop residue production and its contribution to carbon neutrality in China," *Resour. Conserv. Recycl.* 203, article ID 107450. DOI: 10.1016/j.resconrec.2024.107450
- Zuo, M., Le, K., Feng, Y., Xiong, C., Li, Z., Zeng, X., Tang, X., Sun, Y., and Lin, L. (2018). "An effective pathway for converting carbohydrates to biofuel 5-ethoxymethylfurfural via 5-hydroxymethylfurfural with deep eutectic solvents (DESs)," *Industrial Crops and Products*, 112, 18-23. DOI: 10.1016/j.indcrop.2017.11.001

Article submitted: December 28, 2024; Peer review completed: February 8, 2025;
Revised version received: February 15, 2025; Accepted: February 21, 2025; Published:
March 3, 2025,

DOI: 10.15376/biores.20.2.2962-2978